Journal of Sustainable Development of Energy, Water and Environment Systems

http://www.sdewes.org/jsdewes

Year 2020, Volume 8, Issue 3, pp 464-475

Parametric Study of a Single Effect Lithium Bromide-Water Absorption Chiller Powered by a Renewable Heat Source

Muhammad Tawalbeh*[1], Tareq Salameh[2], Mona Albawab[3], Amani Al-Othman[4] Mamdouh El Haj Assad[5], Abdul H. Alami[6]

[1]Sustainable and Renewable Energy Engineering Department, University of Sharjah, P.O. Box 27272, Sharjah, United Arab Emirates
e-mail: mtawalbeh@sharjah.ac.ae

[2]Sustainable and Renewable Energy Engineering Department, University of Sharjah, P.O. Box 27272, Sharjah, United Arab Emirates
e-mail: tsalameh@sharjah.ac.ae

[3]Sustainable and Renewable Energy Engineering Department, University of Sharjah, P.O. Box 27272, Sharjah, United Arab Emirates
e-mail: malbawab@sharjah.ac.ae

[4]Department of Chemical Engineering, American University of Sharjah, P.O. Box 26666, Sharjah, United Arab Emirates
e-mail: aalothman@aus.edu

[5]Sustainable and Renewable Energy Engineering Department, University of Sharjah, P.O. Box 27272, Sharjah, United Arab Emirates
e-mail: massad@sharjah.ac.ae

[6]Sustainable and Renewable Energy Engineering Department, University of Sharjah, P.O. Box 27272, Sharjah, United Arab Emirates
Centre of Advanced Materials Research, University of Sharjah, P.O. Box 27272, Sharjah, United Arab Emirates
e-mail: aalalami@sharjah.ac.ae

Cite as: Tawalbeh, M., Salameh, T., Albawab, M., Al-Othman, A., El Haj Assad, M., Alami, A. H., Parametric Study of a Single Effect Lithium Bromide-Water Absorption Chiller Powered by a Renewable Heat Source, J. sustain. dev. energy water environ. syst., 8(3), pp 464-475, 2020, DOI: https://doi.org/10.13044/j.sdewes.d7.0290

ABSTRACT

This work investigates the performance of a single-effect absorption chiller utilizing an aqueous lithium bromide solution as the working fluid and driven by hot fluid rejected from either a geothermal power plant or the outlet of a thermal solar collector. This relatively low enthalpy return fluid, which will otherwise be reinjected back into the earth, will be utilized as the thermal energy source of the chiller. Although such chillers are considered low-grade energy refrigeration cycles, the one proposed here has an advantage in terms of economy and efficiency. A parametric analysis is performed using Engineering Equation Solver software and is used to highlight the effect of the heat exchanger size on the coefficient of performance of the chiller. The analysis proved that the proposed device can operate with excellent cooling capacity, reaching 16 kW, and a relatively high coefficient of performance (~ 0.7) while being driven by the low-grade energy. The heat source temperature, solution heat exchanger effectiveness and the size of the absorber were shown to be key parameters for the design and operation of absorption chillers. Moreover, increasing the heat source mass flow rate has a significant impact on both cooling capacity and coefficient of performance at low values (< 10 kg/s) and unnoticeable impact at higher values (> 10 kg/s).

* Corresponding author

KEYWORDS

Absorption chiller, Lithium bromide-water, Renewable thermal energy, Parametric study, Refrigeration system, Coefficient of performance.

INTRODUCTION

The geographical location of the United Arab Emirates (UAE) is in the Arabian Peninsula and lies between 22° 30' and 26° 10' north latitude and between 51° and 56° 25' E longitude [1]. This provides a basis for a massive solar exposure. UAE, in particular, receives an annual solar energy incident of 6.3 kWh/m^2/day [2] making UAE of a hot, sub-tropical, and arid climate. Consequently, the energy demand for air conditioning purposes is very high. Nowadays, natural gas and oil are the primary sources of energy in the UAE [3]. The other energy sources are only contributing to around 1% towards the country total energy demand [4]. As the energy prices continue their upward stir, the use of conventional energy sources for air conditioning leads to high electricity bill rates [5]. Moreover, the emissions associated with conventional energy sources have great environmental effects and increasing the threat of global warming [6]. For instance, electricity production is responsible for around 38% of India carbon dioxide (CO_2) emissions where 44% of the electricity is produced by coal-fired power plants and around 27% by other thermal power plants [7]. Hence, an alternative source of energy that is less expensive and does not contribute to environmental pollution is required.

The renewable resources for low-grade thermal energy and are not exclusive to solar thermal collectors. For example, geothermal energy is a green, sustainable and renewable source of energy which is deposited in nature, with almost zero emissions and very minimal side effects. It requires modest land area and low maintenance cost [8]. It can be utilized for many different applications, such as power generation and absorption chiller refrigeration. In absorption chiller, the geothermal energy is utilized as the energy source to provide the heat required for the generator. It lowers the air conditioning cost dramatically where air conditioning is the most electricity consuming process in UAE and accounts for up to 80% of the electricity demand in Abu Dhabi [9].

Geothermal power plants are widely designed as a single-flash steam type [10]. This type is one of the first power plants installed in liquid prevailed geothermal fields. Worldwide, the single flash is the dominant type and stands for 29% and 43% of all geothermal plants and the total capacity of the geothermal power plants installed, respectively. The power capacity is in the range of 3 to 117 MW with an average power rating of about 27 MW [11]. Moreover, normally at least 5-6 productions wells with 2-3 injection wells are needed to run a single-flash power plant of 30 MW [9]. Both medium and low enthalpy resources, on the other hand, can be utilized directly for heating and cooling purposes [12] or in various industrial processes such as food drying, distillation, and desalination [13]. The heating is typically occurred by directly passing the geothermal water through pipes to radiators [14] and absorption chillers are usually employed in cooling applications [15].

Absorption chillers have several advantages when compared to vapor-compression refrigeration cycles. Their cost is lower, they can utilize low-grade heat, natural materials are the working fluids, which do not contribute to the depletion of ozone, and they operate without a compressor, hence, operate with low noise and vibration [16, 17]. As a result, absorption chillers are more economical and eco-friendly.

The most common pairs of working fluid in absorption chillers are lithium bromide-water (LiBr-H_2O) and ammonia-water (NH_3-H_2O) [18]. The LiBr-H_2O pair is more dominant in absorption chillers since it is cheaper, stable, free of toxins and not harmful to the environment [19]. It also has a relatively high latent heat of vaporization, less volatile than water, therefore, a rectifier is not required in the cycle [20]. In addition

to that, LiBr-H_2O absorption chillers have higher Coefficient of Performance (*COP*), operates at low pressures (0.6-8 kPa), relatively high temperatures (5-10 °C), hence, used mainly for air conditioning applications [20]. On the over hand, NH_3-H_2O chillers operate at high pressures (200-50,000 kPA), relatively low temperatures (~ –10 °C) [21], and suffer from toxicity issues and used primarily for refrigeration [22]. In LiBr-H_2O working fluid chillers, LiBr performs as the absorbent, and water acts as the refrigerant [23]. The required heat source temperature for single-effect LiBr-H_2O absorption chiller is between 80 and 100 °C while their *COP* is between 0.7 and 0.8 [24, 25].

Absorption chiller refrigeration cycle consists of seven main components: generator, condenser, two expansion valves, evaporator, absorber, pump and heat exchanger as shown in Figure 1 [26]. There are two main fluids circulating around the system, a refrigerant, and an absorber. A weak refrigerant/absorber solution that is pumped from the low-pressure absorber to the high-pressure generator, passing through the pump and heat exchanger. Inside the generator, heat can be added from many different sources such as solar, geothermal or waste heat. The heat source temperature should be in the range of 80 to 120 °C to evaporate the refrigerant and separate it from the absorbent. The high-pressure vapour is then condensed inside the condenser to saturated liquid. The high-pressure saturated liquid then expands through an expansion valve to lower its pressure and ultimately decrease its temperature as well. The saturated low-pressure liquid refrigerant then enters the evaporator where the liquid is evaporated to a low-pressure vapour. The vapour then enters the absorber to be absorbed by the absorbent. The remaining strong absorber in the generator after being separated from the refrigerant goes back to the absorber. This strong absorber is at high pressure and temperature, hence, it passes through a heat exchanger where it exchanges heat with the solution moving in the opposite direction from the absorber to the generator as shown in Figure 1. The strong absorber then passes through an expansion valve to reduce its pressure to the absorber pressure level.

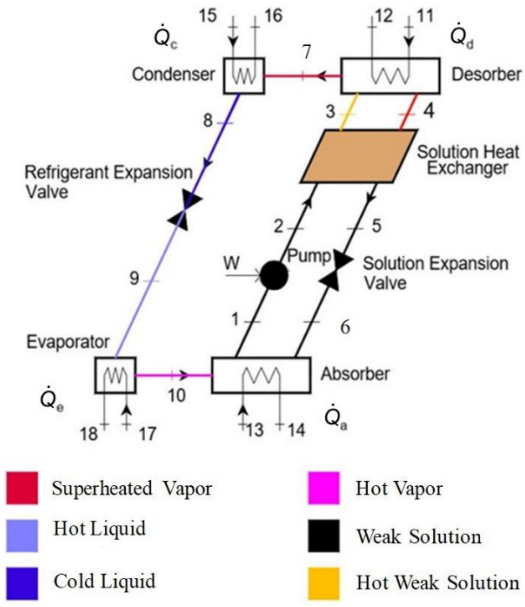

Figure 1. Absorption chiller schematic diagram [26]

Performance, operation, and *COP* of absorption chillers are affected by several parameters such as heat source temperature, heat source, and desorber inlet mass flow rates, desorber and condenser sizes, and solution heat exchanger effectiveness. Hence, the purpose of this work is to perform a parametric study to investigate the effect on the performance and *COP* and to determine the optimum operating parameters of a single

LiBr-H_2O absorption chiller powered by geothermal energy. In the following section, a mathematical model for the absorption chiller system and components is presented.

MATHEMATICAL MODELING

An absorption chiller refrigeration cycle consists of seven main components: a generator (desorber), absorber, evaporator, condenser, solution heat exchanger, solution pump and expansion valve. Neglecting frictional pressure drops, the cycle operates at two pressure levels: high pressure at the generator and condenser, and low pressure at the absorber and evaporator. The LiBr-water solution is the working fluid of choice in the absorber and generator section (absorbent) while water is the working fluid in the evaporator and condenser section (refrigerant). Also, and in order to avoid freezing or solidification inside the evaporator, it is necessary to operate at temperatures slightly above 0 °C.

Several assumptions are made to set up the thermodynamic analysis of LiBr-water absorption chiller:

- All components in the cycle operate at steady state conditions;
- Frictional pressure drops are neglected;
- Pump work is negligible;
- Both expansion valves (pressure reducers) are isentropic;
- The LiBr-water solution exits the absorber and generator and the refrigerant exits the condenser at saturation conditions.

For the current analysis, the mass balance and energy balance equation for each component of absorption chiller are summarized in Table 1. Note that $\dot{Q}$ is the rate of heat transfer, $\dot{m}$ is the mass flow rate, and h is the enthalpy. The subscripts a, c, e, and d represent the absorber, condenser, evaporator, and generator (desorber), respectively. Numerical subscripts from 1 through 18 refer to the streams shown in Figure 1.

Table 1. Summary of mass and energy balance equations for each component of LiBr-water absorption chiller

System component	Mass balance equation	Energy balance equation
Pump	$\dot{m}_1 = \dot{m}_2$	$\dot{w} = \dot{m}_2 h_2 - \dot{m}_1 h_1$
Solution heat exchanger	$\dot{m}_2 = \dot{m}_3$ $\dot{m}_4 = \dot{m}_5$	$\dot{m}_2 h_2 + \dot{m}_4 h_4 = \dot{m}_3 h_3 + \dot{m}_5 h_5$
Solution expansion valve	$\dot{m}_5 = \dot{m}_6$	$\dot{m}_5 h_5 = \dot{m}_6 h_6$ $h_5 = h_6$
Absorber	$\dot{m}_1 = \dot{m}_6 + \dot{m}_{10}$	$\dot{Q}_\mathrm{a} = \dot{m}_6 h_6 + \dot{m}_{10} h_{10} - \dot{m}_1 h_1$
Desorber (generator)	$\dot{m}_3 = \dot{m}_4 + \dot{m}_7$	$\dot{Q}_\mathrm{d} = \dot{m}_4 h_4 + \dot{m}_7 h_7 - \dot{m}_3 h_3$
Condenser	$\dot{m}_7 = \dot{m}_8$	$\dot{Q}_\mathrm{c} = \dot{m}_7 h_7 - \dot{m}_8 h_8$
Refrigerant expansion valve	$\dot{m}_8 = \dot{m}_9$	$\dot{m}_8 h_8 = \dot{m}_9 h_9$ $h_8 = h_9$
Evaporator	$\dot{m}_9 = \dot{m}_{10}$	$\dot{Q}_\mathrm{e} = \dot{m}_{10} h_{10} - \dot{m}_9 h_9$

The rate of heat transfer in the absorber, condenser, evaporator, and generator are estimated. The equations are listed as follows:

- Absorber:

$$\dot{Q}_\mathrm{a} = \dot{m}_{13} c_\mathrm{p} \left(T_{14} - T_{13} \right) \tag{1}$$

$$\dot{Q}_{\mathrm{a}} = (UA)_{\mathrm{a}} \frac{(T_6 - T_{14}) - (T_1 - T_{13})}{\ln\left(\frac{T_6 - T_{14}}{T_1 - T_{13}}\right)} \tag{2}$$

- Condenser:

$$\dot{Q}_{\mathrm{a}} = \dot{m}_{15} c_{\mathrm{p}} (T_{16} - T_{15}) \tag{3}$$

$$\dot{Q}_{\mathrm{c}} = (UA)_{\mathrm{c}} \frac{(T_{15} - T_8) - (T_{16} - T_7)}{\ln\left(\frac{T_{15} - T_8}{T_{16} - T_7}\right)} \tag{4}$$

- Evaporator:

$$\dot{Q}_{\mathrm{e}} = \dot{m}_{17} c_{\mathrm{p}} (T_{17} - T_{18}) \tag{5}$$

$$\dot{Q}_{\mathrm{e}} = (UA)_{\mathrm{e}} \frac{(T_{17} - T_{10}) - (T_{18} - T_9)}{\ln\left(\frac{T_{17} - T_{10}}{T_{18} - T_9}\right)} \tag{6}$$

- Desorber (generator):

$$\dot{Q}_{\mathrm{e}} = \dot{m}_{11} c_{\mathrm{p}} (T_{11} - T_{12}) \tag{7}$$

$$\dot{Q}_{\mathrm{d}} = (UA)_{\mathrm{d}} \frac{(T_{11} - T_4) - (T_{12} - T_7)}{\ln\left(\frac{T_{11} - T_4}{T_{12} - T_7}\right)} \tag{8}$$

where T is the temperature, U [W/m^{2}K] is the overall heat transfer coefficient, A [m^2] is the area and c_{p} [kJ/kgK] is the specific heat for the stream of interest. The ratio of the actual heat transfer rate and the maximum possible heat transfer rate is the effectiveness (ε) of the solution heat exchanger. It is expressed as:

$$\varepsilon = \frac{\dot{m}_4 c_{\mathrm{p}} (T_4 - T_5)}{(\dot{m} c_{\mathrm{p}})_{\min} (T_4 - T_2)} \tag{9}$$

Due to the evaporation in the generator, the heat capacitance ($\dot{m}_4 c_{\mathrm{p}}$) is always lower than $\dot{m}_3 c_{\mathrm{p}}$, and the effectiveness can be written as:

$$\varepsilon = \frac{T_4 - T_5}{T_4 - T_2} \tag{10}$$

Finally, the *COP* for the absorption chiller is defined as:

$$COP = \frac{\dot{Q}_{\mathrm{e}}}{\dot{Q}_{\mathrm{d}}} \tag{11}$$

The mass and energy balance equations are then solved using the set of the input parameters shown in Table 2. The parameters are fluid flow rates, inlet temperatures, heat exchangers, overall heat transfer coefficients and heat exchangers sizes. The full thermodynamic analysis is carried out via Engineering Equation Solver software (EES) where all physical and thermal properties were extracted from the software library. In parallel, several manual calculations were done to verify the EES analysis using the same mass and energy balance equations. Supplemental data available in the enthalpy versus concentration chart and Duhring chart of crystallization for $LiBr/H_2O$ solution shown in Figure 2 were also used.

Table 2. Input parameters for mass and energy balance equations

Input parameter	Value	Input parameter	Value
$(UA)_d$	1.0 kW/K	$\dot{m}_{13}$	0.28 kg/s
$(UA)_a$	1.8 kW/K	$\dot{m}_{15}$	0.28 kg/s
$(UA)_c$	1.2 kW/K	$\dot{m}_{17}$	0.4 kg/s
$(UA)_e$	2.25 kW/K	T_{13}	25 °C
$\dot{m}_1$	0.05 kg/s	T_{15}	25 °C
$\dot{m}_{11}$	1 kg/s	T_{17}	10 °C

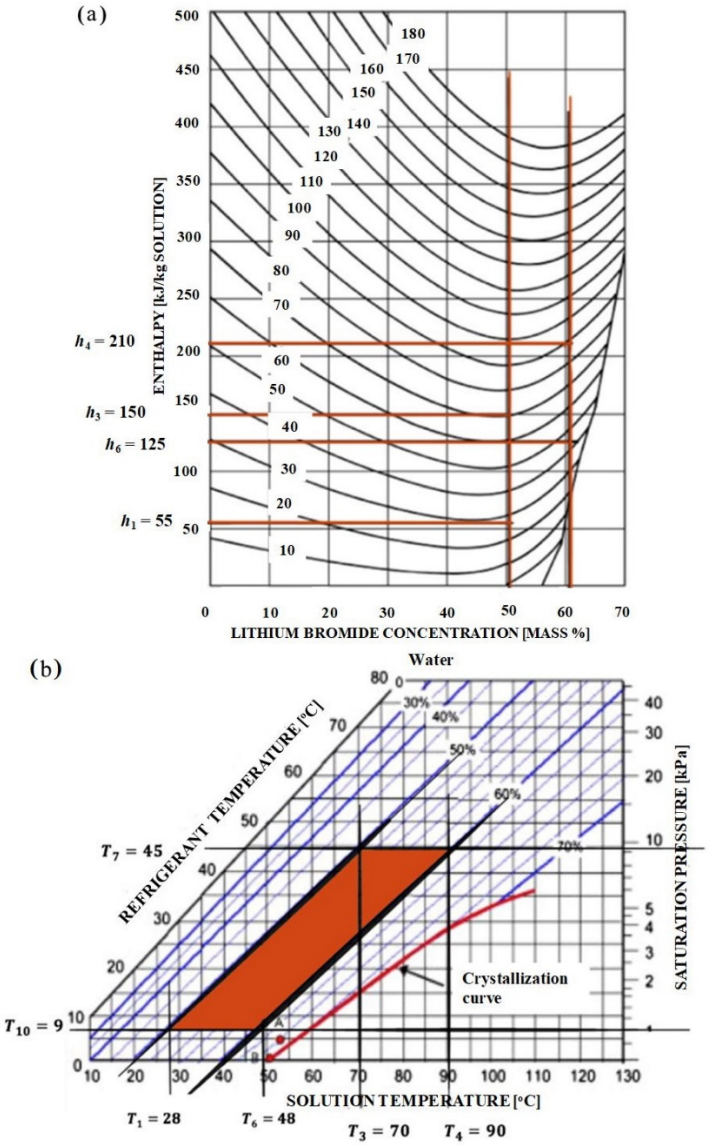

Figure 2. Enthalpy vs. concentration (a) and Duhring chart of crystallization plot for $LiBr$-H_2O solution (b) [27, 28]

RESULTS AND DISCUSSION

In the following sections, the effect of several process variables on the cooling capacity and *COP* will be discussed. These variables include: the effect of the desorber inlet temperature, effect of the heat source inlet mass flow rate and the effect of the absorber heat exchanger size.

Effect of desorber inlet temperature

The thermal source to the chiller is the hot fluid exiting a low-enthalpy renewable resource, such as a geothermal power plant and into the rejection well. The temperature of this heat source is an important parameter having a significant influence on the performance and operation of the refrigeration cycle. To operate the sought single effect LiBr-water absorption chiller, the temperature of this stream should be at least at 90 °C. This condition is easily achieved by the rejected hot fluid from a geothermal power plant. This effect is evident in Figure 3 that show the effect of desorber inlet temperature (designated by T_{11}), at different solution heat exchanger effectiveness (ε) and at fixed heat source mass flow rate of 1 kg/s, on the performance of the refrigeration cycle represented by the cooling capacity ($\dot{Q}_e$). A similar analysis is shown in Figure 4 but shows the effect on *COP*. The correlation in Figure 3 shows similar trends for various mass flow rate levels, with the cooling capacity decreasing with increased flow rate due to the shortened residence time of the working fluid in the heat exchangers. The cooling capacity of the chiller is seen to increase as the inlet heat temperature increases in a fashion consistent. This can be explained by the increase of the log mean temperature difference of each heat exchanger. However, this increase of log mean temperature difference results in an increase in the irreversibility in the real heat exchanger. This may explain the behaviour of the *COP* with the increase of the temperature of the heat sources.

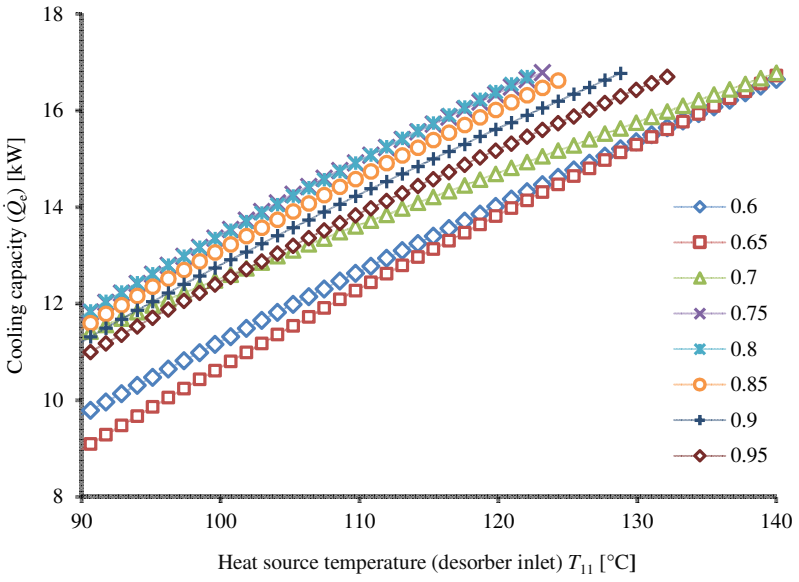

Figure 3. Effect of the heat source temperature on the cooling capacity ($\dot{Q}_e$) at different solution heat exchanger effectiveness values at desorber inlet mass flow rate of 1 kg/s

The *COP* values in Figure 4 is observed to decrease with increasing the heat source temperature in the range between 90 to 140 °C. In reality, the *COP* would increase first then reach an inflection point where maximum value is achieved decreasing again [29]. This increase is usually observed at temperature ranges below 90 °C, which is not included in the current study. The temperature range considered here mimics temperature of the hot fluid rejected back by the geothermal power plant to its rejection well.

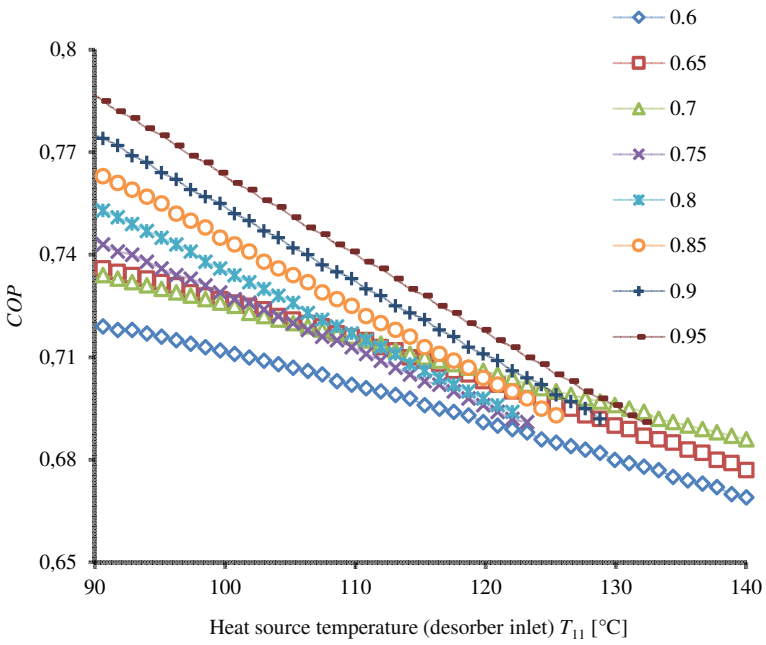

Figure 4. Effect of heat source temperature on *COP* at different solution heat exchanger effectiveness values at desorber inlet mass flow rate of 1 kg/s

Effect of the heat source inlet mass flow rate

Figure 5 show the effect of the mass flow rate of the heat source ($\dot{m}_{11}$) on the cooling capacity while fixing the solution heat exchanger effectiveness at 0.65. The heat source inlet mass flow rate was varied from 1 kg/s to 50 kg/s at increments of 10 kg/s with the solution heat exchanger effectiveness value of 0.65. It is evident that the cooling load increases by increasing the mass flow rate from 1 kg/s to and 10 kg/s. However, there was no noticeable change in the mass flow rate between 10 kg/s and 50 kg/s. On the other hand, *COP* slightly decreased by increasing the heat source inlet mass flow rate from 1 kg/s to and 10 kg/s, whereas no noticeable change was observed by increasing the mass flow rate between 10 kg/s and 50 kg/s as clearly seen in Figure 6.

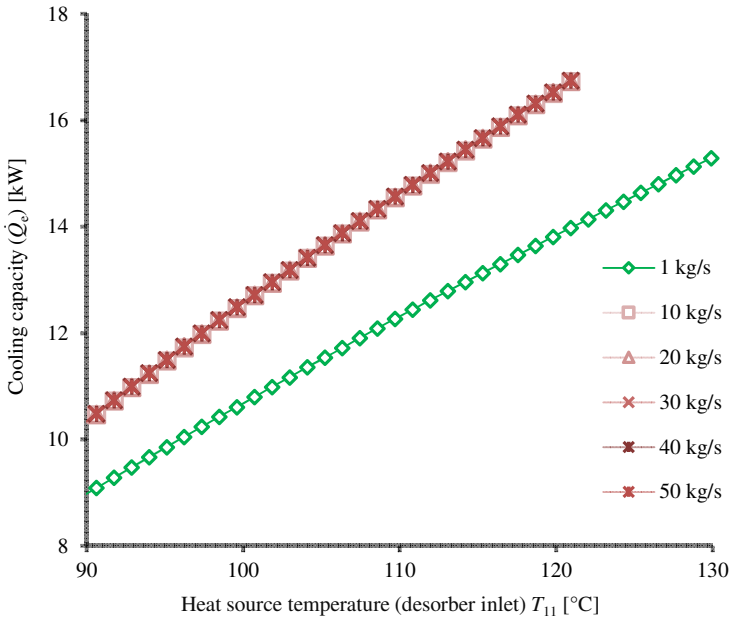

Figure 5. Effect of heat source temperature on cooling capacity ($\dot{Q}_e$) at different desorber inlet mass flow rate and solution heat exchanger effectiveness of 0.65

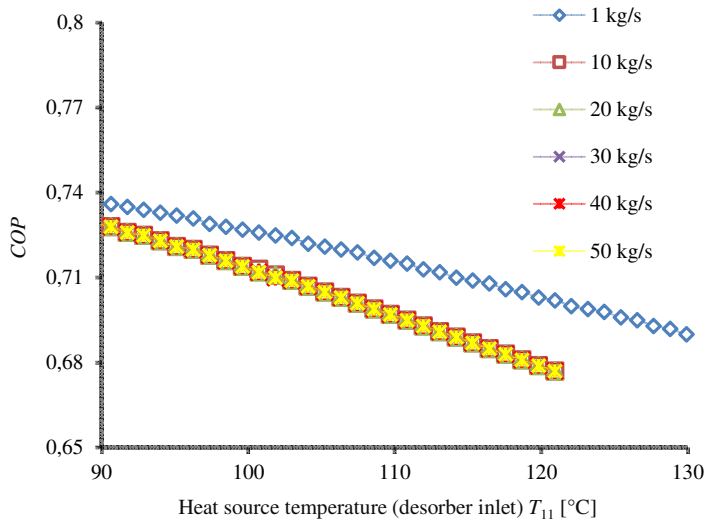

Figure 6. Effect of heat source temperature on *COP* at different desorber inlet mass flow rate and solution heat exchanger effectiveness of 0.65

The chiller performance strongly correlates with the size of the solution heat exchanger, represented by its effectiveness. Thus, it is extremely difficult to explicitly reveal any effect of the heat source mass flow rate change on the chiller performance as long as the size of the solution heat exchanger is the same. This is further explored in the next section.

Effect of the absorber heat exchanger size

The effect of the absorber heat exchanger size on the cooling capacity and *COP* of the absorption chiller at different heat source temperatures is demonstrated in Figure 7 and Figure 8, respectively. The effectiveness of the heat exchanger was kept constant at 0.65. The size of the absorber heat exchanger is represented by the *UA* values. It is evident from Figure 7 and Figure 8 that the cooling capacity and *COP* are increasing exponentially with increasing the size of the absorber heat exchanger (UA_a) for all heat source temperatures. This increase of the cooling capacity and *COP* is very high at low values of *UA*'s up to 1.6 and less noticeable at higher values of *UA*'s. Hence, any increase of UA_a above the value of 1.6 is not justified economically.

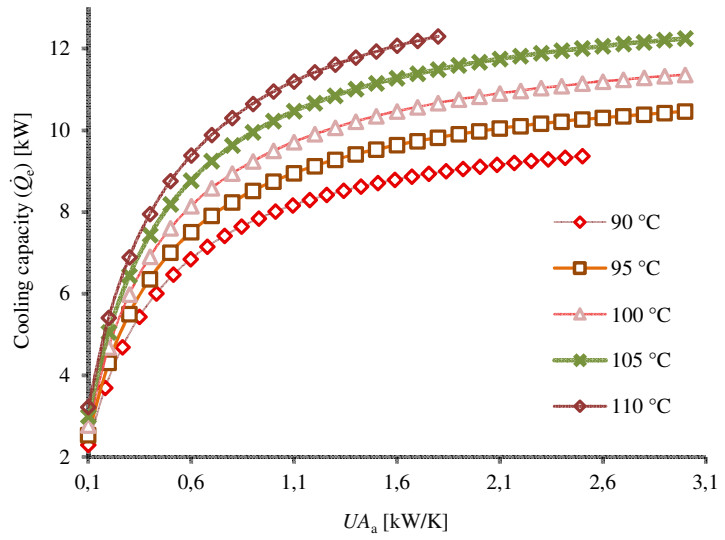

Figure 7. Effect of the absorber size on the cooling capacity ($\dot{Q}_e$) at solution heat exchanger effectiveness of 0.65 and different heat source inlet temperature

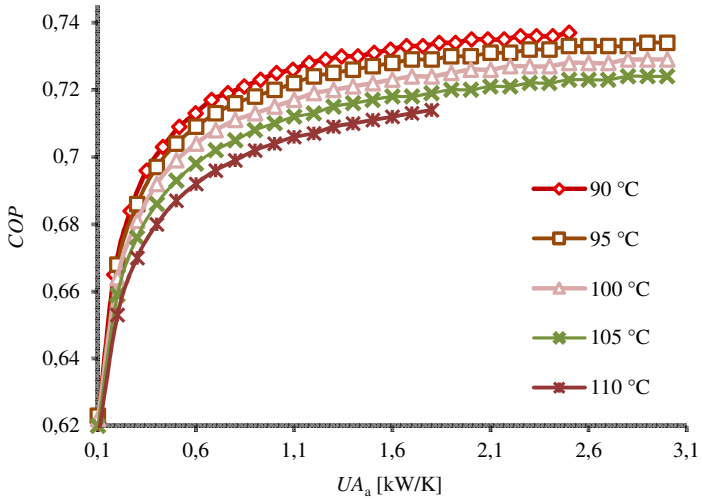

Figure 8. Effect of the absorber size on the *COP* at solution heat exchanger effectiveness of 0.65 and different heat source inlet temperature

CONCLUSIONS

This work analyzed the performance of single-effect LiBr-water absorption chiller driven by the hot fluid rejected back by a low enthalpy thermal renewable resource, such as a geothermal power plant. The parametric study was conducted using the EES. The results showed that absorption chillers could operate with an acceptable *COP* and cooling capacity using low-grade energy with minimum noise. The parametric study verified the effect of the several parameters including the heat source temperature and its mass flow rate, solution heat exchanger effectiveness and the size of the absorber heat exchanger. For example, it was evident that the cooling load increased by increasing the heat source mass flow rate from 1 kg/s to and 10 kg/s, while the *COP* has slightly decreased. Furthermore, the increase in the heat source mass flow rate is significant at low mass flow rate values (< 10 kg/s) and unnoticeable at higher mass flow rate values (> 10 kg/s). While the previous process variables are key parameters for the design and operation of absorption chillers, however, further studies are needed in the future to examine wider ranges of operating conditions such as mass flow rate of the working fluid, renewable resource exit temperature range, renewable resource availability, among others.

NOMENCLATURE

A	area	[m^2]
c_p	specific heat	[kJ/kgK]
h	specific enthalpy	[kJ/kg]
$\dot{m}$	mass flow rate	[kg/s]
$\dot{Q}$	rate of heat transfer	[kW]
T	temperature	[°C]
U	the overall heat transfer coefficient	[W/m^2K]

Greek letters

ε	heat exchanger effectiveness

Subscripts

a	absorber
c	condenser
d	desorber
e	evaporator

Abbreviations

COP Coefficient of Performance
EES Engineering Equation Solver software

REFERENCES

1. Mokri, A., Ali, M. A. and Emziane, M., Solar Energy in the United Arab Emirates: A Review, *Renewable and Sustainable Energy Reviews*, Vol. 28 pp 340-375, 2013, https://doi.org/10.1016/j.rser.2013.07.038
2. Al-Othman, A., Tawalbeh, M., El Haj Asaad, M., Alkayyali, T. and Eisa, A., Novel Multi-Stage Flash (MSF) Desalination Plant Driven by Parabolic Trough Collectors and a Solar Pond: A Simulation Study in UAE, *Desalination*, Vol. 443, pp 237-244, 2018, https://doi.org/10.1016/j.desal.2018.06.005
3. Alami, A. H., Aokal, K., Zhang, D., Tawalbeh, M., Alhammadi, A. and Taieb, A., Assessment of Calotropis Natural Dye Extracts on the Efficiency of Dye-Sensitized Solar Cells, *Agronomy Research*, Vol. 16, No. 4, pp 1569-1579, 2018, https://doi.org/10.15159/ar.18.166
4. Kazim, A. M., Assessments of Primary Energy Consumption and its Environmental Consequences in the United Arab Emirates, *Renewable Sustainable Energy Reviews*, Vol. 11, No. 3, pp 426-446, 2007, https://doi.org/10.1016/j.rser.2005.01.008
5. International Renewable Energy Agency (IRENA), REProspects UAE, Remap 2030, 2015.
6. Foley, A. and Olabi, A. G., Renewable Energy Technology Developments, Trends and Policy Implications that Can Underpin the Drive for Global Climate Change, *Renewable and Sustainable Energy Reviews*, Vol. 68, Part 2, pp 1112-1114, 2017, https://doi.org/10.1016/j.rser.2016.12.065
7. Singhal, T. and Manjare, S. D., Modelling Studies on Reactive Absorption of Carbon Dioxide in Monoethanolamine Solution from Flue Gas in Coal Based Thermal Power Plants, *Journal of Sustainable Development of Energy, Water and Environment Systems*, Vol. 6, No. 3, pp 481-493, 2018, https://doi.org/10.13044/j.sdewes.d6.0227
8. El Haj Assad, M., Bani-Hani, E. and Khalil, M., Performance of Geothermal Power Plants (Single, Dual, and Binary) to Compensate for LHC CERN Power Consumption: Comparative Study, *Geothermal Energy*, Vol. 5, pp 17, 2017, https://doi.org/10.1186/s40517-017-0074-z
9. Giusti, L. and Almoosawi, M., Impact of Building Characteristics and Occupants' Behaviour on the Electricity Consumption of Households in Abu Dhabi (UAE), *Energy and Buildings*, Vol. 151, pp 534-547, 2017, https://doi.org/10.1016/j.enbuild.2017.07.019
10. Lee, K. C., Classification of Geothermal Resources by Exergy, *Geothermics*, Vol. 30, No. 4, pp 431-442, 2001, https://doi.org/10.1016/S0375-6505(00)00056-0
11. DiPippo, R., *Geothermal Power Plants: Principles, Applications, Case Studies and Environmental Impact* (3rd ed.), Chapter 5 (pp 82-109), Butterworth-Heineman, Oxford, UK, 2012.
12. Chua, K. J., Chou, S. K. and Yang, W. M., Advances in Heat Pump Systems: A Review, *Applied Energy*, Vol. 87, No. 12, pp 3611-3624, 2010, https://doi.org/10.1016/j.apenergy.2010.06.014
13. Yilmaz, C., Thermodynamic and Economic Investigation of Geothermal Powered Absorption Cooling System for Buildings, *Geothermics*, Vol. 70, pp 239-248, 2017, https://doi.org/10.1016/j.geothermics.2017.06.009
14. Koziol, J. and Mendecka, B., Evaluation of Economic, Energy-environmental and Sociological Effects of Substituting Non-renewable Energy with Renewable Energy Sources, *Journal of Sustainable Development of Energy, Water and Environment Systems*, Vol. 3, No. 4, pp 333-343, 2015, https://doi.org/10.13044/j.sdewes.2015.03.0025

15. Lund, J. W., Direct Utilization of Geothermal Energy, *Energies*, Vol. 3, No. 8, pp 1443-1471, 2010, https://doi.org/10.3390/en3081443
16. Kaynakli, O. and Kilic, M., Theoretical Study on the Effect of Operating Conditions on Performance of Absorption Refrigeration System, *Energy Conversion and Management*, Vol. 48, No. 2, pp 599-607, 2007, https://doi.org/10.1016/j.enconman.2006.06.005
17. Shirazi, A., Taylor, R. A., Morrison, G. L. and White, S. D., Solar-Powered Absorption Chillers: A Comprehensive and Critical Review, *Energy Conversion and Management*, Vol. 171, pp 59-81, 2018, https://doi.org/10.1016/j.enconman.2018.05.091
18. Berdasco, M., Coronas, A. and Valles, M., Study of the Adiabatic Absorption Process in Polymeric Hollow Fiber Membranes for Ammonia/Water Absorption Refrigeration Systems, *Applied Thermal Engineering*, Vol. 137, pp 594-607, 2018, https://doi.org/10.1016/j.applthermaleng.2018.04.004
19. Raja, V. B. and Shanmugam, V., A Review and New Approach to Minimize the Cost of Solar Assisted Absorption Cooling System, *Renewable and Sustainable Energy Reviews*, Vol. 16, No. 9, pp 6725-6731, 2012, https://doi.org/10.1016/j.rser.2012.08.004
20. Somers, C., Mortazavi, A., Hwang, Y., Radermacher, R., Rodgers, P. and Al-Hashimi, S., Modeling Water/Lithium Bromide Absorption Chillers in ASPEN Plus, *Applied Energy*, Vol. 88, No. 11, pp 4197-4205, 2011, https://doi.org/10.1016/j.apenergy.2011.05.018
21. Padilla, R. V., Demirkaya, G., Goswami, D. Y., Stefanakos, E. and Rahman, M. M., Analysis of Power and Cooling Cogeneration Using Ammonia-Water Mixture, *Energy*, Vol. 35, No. 12, pp 4649-4657, 2010, https://doi.org/10.1016/j.energy.2010.09.042
22. Boudehenn, F., Demasles, H., Wyttenbach, J., Jobard, X., Cheze, D. and Papillon, P., Development of a 5 Kw Cooling Capacity Ammonia-Water Absorption Chiller for Solar Cooling Applications, *Energy Procedia*, Vol. 30, pp 35-43, 2012, https://doi.org/10.1016/j.egypro.2012.11.006
23. Zhai, X. Q., Qu, M., Li, Y. and Wang, R. Z., A Review for Research and New Design Options of Solar Absorption Cooling Systems, *Renewable and Sustainable Energy Reviews*, Vol. 15, No. 9, pp 4416-4423, 2011, https://doi.org/10.1016/j.rser.2011.06.016
24. Gomri, R., Investigation of the Potential of Application of Single Effect and Multiple Effect Absorption Cooling Systems, *Energy Conversion and Management*, Vol. 51, No. 9, pp 1629-1636, 2010, https://doi.org/10.1016/j.enconman.2009.12.039
25. Lake, A., Rezaie, B. and Beyerlein, S., Use of Exergy Analysis to Quantify the Effect of Lithium Bromide Concentration in an Absorption Chiller, *Entropy*, Vol. 19, No. 4, pp 156-171, 2017, https://doi.org/10.3390/e19040156
26. El Haj Assad, M., Tawalbeh, M., Salameh, T. and Al-Othman, A., Thermodynamic Analysis of Lithium Bromide Absorption Chiller Driven by Geothermal Energy, *Proceedings of the 5th International Conference on Renewable Energy: Generation and Applications (ICREGA'18)*, pp 76-81, Al Ain, United Arab Emirates, 2018.
27. Verma, A., Satish and Chakraborty, P. R., Water-Lithium Bromide Absorption Chillers for Solar Cooling, in: *Applications of Solar Energy (Energy, Environment, and Sustainability)*, Springer, Singapore, 2018.
28. Herold, K. E., Radermacher, R. and Klein S. A., *Absorption Chillers and Heat Pumps*, CRC Press, Boca Raton, Florida, USA, 2016, https://doi.org/10.1201/b19625
29. Al-Tahaineh, H., Frihat, M. and Al-Rashdan, M., Exergy Analysis of a Single-Effect Water-Lithium Bromide Absorption Chiller Powered by Waste Energy Source for Different Cooling Capacities, *Energy and Power*, Vol. 3, No. 6, pp 106-118, 2013, https://doi.org/10.5923/j.ep.20130306.02

Paper submitted: 14.02.2019
Paper revised: 07.05.2019
Paper accepted: 14.06.2019